Journal of Engineering and Technology for Industrial Applications

ISSN ONLINE: 2447-0228

ITEGAM-JETIA

Manaus, v.11 n.55, p. 128-139. September/October., 2025.
DOI: https://doi.org/10.5935/jetia. v11i55.2513

RESEARCH ARTICLE OPEN ACCESS

RISK QUANTIFICATION IN MANUFACTURING INDUSTRY INVESTMENTS: A STOCHASTIC APPROACH WITH ARTIFICIAL INTELLIGENCE

Rafael Vieira da Silva[1], Enzo Morosini Frazzon[2]

[1, 2,] Production and Systems Engineering Department, Federal University of Santa Catarina, Florianópolis, Brazil

[1]https://orcid.org/0009-0001-0581-0008, [2]https://orcid.org/0000-0002-6629-6938

Email: rafael.vieira@dep.eng.br, enzo.frazzon@gmail.com

ARTICLE INFO

Article History
Received: August 14, 2025
Revised: August 20, 2025
Accepted: September 15, 2025
Published: September 30, 2025

Keywords:
Investments,
Supply Chain,
Risk Evaluation,
Techno-Economic Feasibility,
Decision-Making Methods.

ABSTRACT

Manufacturing investment decisions are often hindered by significant uncertainty. This paper introduces a conceptual model that integrates stochastic simulation with machine learning to quantify investment risk. Our hybrid approach employs a Monte Carlo simulation using time series data of fixed, variable, and investment costs as inputs. To enhance the simulation's realism, Long Short-Term Memory (LSTM) recurrent neural networks forecast the trend components of these series, while a Vector Autoregression (VAR) model captures their inter-correlations. This framework generates a multitude of potential scenarios, each evaluated through a mathematical model of the supply chain to produce a distinct cash flow. The subsequent application of investment metrics, such as Net Present Value (NPV) and Discounted Payback, to the distribution of these cash flows enables a comprehensive statistical analysis of the investment's risk profile, thereby providing robust support for strategic decision-making.

Copyright ©2025 by authors and Galileo Institute of Technology and Education of the Amazon (ITEGAM). This work is licensed under the Creative Commons Attribution International License (CC BY 4.0).

I. INTRODUCTION

Investment risks in the manufacturing industry are significant due to various intrinsic characteristics of the production chain. The central position of the manufacturing sector within the supply chain makes it particularly sensitive to fluctuations in the supply of raw materials and changes in demand. This sensitivity is further intensified by the highly specialized nature of its production processes [1]. Consequently, structural changes in the supply chain often require substantial investments to adapt production processes. In addition to these factors, a wide range of risks can affect the supply chain, including regulatory changes, natural disasters, disruptions in logistics systems, shifts in consumer preferences, wars, and deliberate attacks on industrial infrastructure. These events are often unpredictable and their consequences uncontrollable [2].

Despite the high level of risk, investments in the supply chain are essential for maintaining competitiveness and meeting market demands. This creates a duality between the inherent risk of investing and the necessity of doing so [3], [4]. Therefore, investments in the manufacturing industry require extensive planning, encompassing a minimum time horizon to ensure return on investment. Motivated by this need, several researchers have developed methods for quantifying investment risks and supporting decision-making [5]. Among these efforts, stochastic approaches have stood out for assessing investment risks. However, there remains a research gap regarding the application of neural network tools for this purpose [6](submitted for publication). This integration is essential, as artificial intelligence techniques excel at identifying patterns, while stochastic methods are particularly effective in analyzing scenarios under uncertainty. The current context is especially conducive to the development of such approaches, due to advances in computational capabilities, improvements in programming libraries and languages, and the growing popularity of artificial intelligence.

Given this context, this study proposes a conceptual model that integrates neural networks and stochastic methods to quantify investment risks in the manufacturing industry. This paper is organized as follows: Chapter II presents the theoretical background of the components of the model; Chapter III introduces the proposed conceptual model; Chapter IV provides the results and discussions approach; and Chapter V provides the concluding remarks. This study is limited to the proposal of a conceptual model, presenting its structure, tools, and implementation methods. However, the implementation of the proposed method is beyond the scope of this article and will be addressed in future research.

II. THEORETICAL REFERENCE

II.1 MONTE CARLO METHOD

The Monte Carlo method is a computational approach based on simulations generated from random numbers applied to probabilistically defined models. It has proven effective in analyzing complex systems where deterministic models are infeasible or inaccurate. Its flexibility and ability to handle uncertainty have made it widely adopted in various fields [7]. For instance, it is used in finance for pricing financial options, portfolio evaluation, and risk analysis; in engineering for system reliability assessment and maintenance planning [8], [9]; and in computer science for high-dimensional integration and machine learning algorithms [10], [11].

For investment risk assessment in the manufacturing industry, the Monte Carlo method can handle volatility in commodity prices, finished goods, and operational costs. This flexibility in modeling multiple variables is crucial in sensitive environments such as investment evaluation. Its strength becomes even more evident when integrated with other methods, such as Vector Autoregression (VAR), enabling multivariate analyses [12]. Correlation analyses between variables are essential for investment assessment, especially considering the interdependence of products within supply chains [13]. Given that uncertainty in time series tends to increase over time, Monte Carlo simulations are well-suited for long-term projections, as they naturally account for increasing volatility [14].

The Monte Carlo method typically follows a systematic structure that may vary by context but often includes: problem definition, statistical analysis, random number generation, scenario simulation, and result analysis [15]. The process begins by defining the scope and identifying initial parameters and variables. Statistical analysis includes data collection, preliminary analysis, and fitting statistical distributions. To incorporate uncertainty, random numbers are generated according to these distributions [16]. Each set of random numbers produces a new simulated scenario. Simulation results are compiled to compute metrics such as mean, median, variance, and confidence intervals [15], [16]. In the context of time series analysis, a typical Monte Carlo modeling approach involves decomposing the series into trend, seasonality, and residual components, as expressed in Equation 1:

Monte Carlo Equation

$$\mathrm{Y_t} = Trend_t + Seasonality_t + X_t \tag{1}$$

Where: The $Trend_t$ represents the systematic behavior of a variable, ignoring cyclical variations and noise. It can be modeled using linear, exponential, polynomial trends, or more advanced methods such as neural networks [17]; The $Seasonality_t$ refers to predictable, cyclic components of the time series, often linked to natural, social, or economic events. Unlike trends and residuals, seasonality occurs at fixed intervals (e.g., days, months, years) [17], And the Residuals (X_t) capture unpredictable variations not explained by trend or seasonality. These components reflect external or internal conditions and exhibit no clear periodicity or dependency over time [17]. If residuals follow a normal distribution, they can be modeled as white noise – $\epsilon_t \sim N(0, \sigma^2)$. For highly volatile systems with cumulative noise, Brownian noise (or Brownian motion) is more appropriate, as it better describes the long-term stochastic behavior of asset time series. As shown in Equation 2 the noise at time t is the sum of white noise and the accumulated noise from the previous time step [18].

Brownian Motion Equation

$$X_t = X_{t-1} + \epsilon_t \tag{2}$$

Where:
X_t: noise value at time t;
X_{t-1}: noise value at time $t-1$;
ϵ_t: white noise at time t.

II.2 TIME SERIES DECOMPOSITION

Each time series component must be treated individually in the analytical process. Therefore, decomposing the time series into trend, seasonality, and noise components is essential. One effective method for this task is STL decomposition (Seasonal and Trend decomposition using Loess), which presents several advantages: robustness to non-stationary data, flexibility in handling complex seasonal patterns, resistance to noise and structural changes, and the direct extraction of trend, seasonality, and residual components through iterative optimization [19], [20]. However, it requires careful parameter tuning, entails higher computational complexity, assumes constant seasonality, and may encounter limitations with very short or very long time series [21].

The STL decomposition process begins by defining the cycle length of the time series. For monthly data, the cycle is typically annual, resulting in a period of 12 months. Equation 3 calculates the initial seasonal component, which serves as the basis for the first iteration. This involves summing all observations that occur in the same position within each cycle (e.g., every January), and dividing by the number of complete cycles. The next step involves centering the initial seasonal values using Equation 4, which removes bias and ensures that the seasonal component does not interfere with other components of the time series.

Initial Seasonality Equation

$$S_i = \frac{1}{N}\sum_{t \in \text{ciclo i}} Y_t \tag{3}$$

Centered Seasonality Equation

$$S_t = S_i - \frac{1}{p}\sum_{i=1}^{p} S_i \tag{4}$$

Where:

S_i: estimated seasonal component at position i within the cycle;
N: total number of complete cycles in the time series;
Y_t: value at time t;
p: number of periods within one cycle.

The trend is calculated by subtracting the seasonal component from the original series, as shown in Equation 5 resulting in the adjusted series Yt', which contains both noise and trend. The Loess method is then applied to Yt' to remove the noise and extract the smoothed trend component, as shown in Equation 6.

Time Series less Seasonality Equation

$$Y_t^{'} = Y_t - S_t \tag{5}$$

Trend Loess Equation

$$T_t = \text{Loess}\left(Y_t^{'}\right) \tag{6}$$

Since the initial seasonal estimate may include elements of trend and noise, STL applies Equation 7 to subtract the extracted trend from the original time series, yielding the intermediate series $Y_t^{''}$. Loess is then applied again to this intermediate series to refine the seasonal component, as shown in Equation 8 [22].

Time Series less Tend Equation

$$Y_t^{''} = Y_t - T_t \tag{7}$$

Seasonality Loess Equation

$$S_t = \text{Loess}\left(Y_t^{''}, \text{periodicity } p\right) \tag{8}$$

The residual component (noise) is calculated by subtracting both trend and seasonal components from the original time series, as given in Equation 9. STL is an iterative method, and Equations 5 through Equation 9 must be repeated iteratively, where *k* represent the current iteration.

White Noise Equation

$$\epsilon_t = Y_t - T_t - S_t \tag{9}$$

Max Error Equation

$$(\sum \epsilon_t^2)^k - (\sum \epsilon_t^2)^{-k} > \ Error_{max} \tag{10}$$

The number of iterations can be adjusted based on criteria such as the threshold defined by Equation 10, where the stopping condition is determined by the difference in the sum of squared residuals between two consecutive iterations. Additional parameters may also be set, such as a maximum number of iterations, in order to stop the process in cases of non-convergence [22].

II.3 RECURRENT NEURAL NETWORKS AND LSTM

The architecture of traditional multilayer perceptrons (MLPs) includes a fixed number of input neurons defined by the dataset's dimensionality. Each input is connected to all neurons in the hidden layers, which means the data is processed independently - ignoring the temporal structure of sequential data [23]. Furthermore, traditional networks lack memory mechanisms and cannot retrieve previous computations, making them unsuitable for tasks such as time series modeling or natural language processing. To address these limitations, Recurrent Neural Networks (RNNs) were introduced by David Rumelhart, Geoffrey Hinton, and Ronald J. Williams in the 1980s [24]. Despite improvements over traditional networks, RNNs face training challenges when dealing with long sequences. Recurrent weights are multiplied across many time steps, leading to vanishing or exploding gradients, which hinder convergence [25], [26].

To address this, Sepp Hochreiter and Jürgen Schmidhuber proposed the Long Short-Term Memory (LSTM) network in 1997, introducing the concepts of cell state and gates [26]. The cell state and hidden state give LSTM the ability to store both long- and short-term dependencies - often referred to as the network's "memory." Gates, typically controlled by sigmoid activations, act as dynamic weights that determine which information to retain, discard, or update. These innovations make LSTM networks more robust against gradient problems and capable of adaptively learning patterns in sequential data [27].

Mathematically, the forget gate is defined in Equation 11, controlling how much of the previous cell state is retained. Simultaneously, the input gate (Equation 12) and candidate cell state (Equation 13) determine the contribution of new information. The updated cell state is calculated using Equation 14.

Forget Gate Equation

$$f_t \ = \ \sigma(w_f[h_{t-1}, x_t)] + b_f) \tag{11}$$

Input Gate Equation

$$i_t = \sigma(w_i[h_{t-1}, x_t)] + b_i) \tag{12}$$

Candidate Cell State Equation

$$\widetilde{C_t} = tanh(w_{\tilde{C}}[h_{t-1}, x_t] + b_{\tilde{C}}) \quad (13)$$

Updated Cell State Equation

$$C_t = f_t \odot C_{t-1} + i_t \odot \widetilde{C_t} \quad (14)$$

Where:

σ: sigmoid function;
w: gate weight;
b: bias weight;
tanh: tanh function.
$\odot$: element-wise multiplication.

The hidden state reflects the current output of the LSTM cell and is calculated using Equation 15, combining the output gate (Equation 16) and the updated cell state:

Output Gate Equation

$$o_t = \sigma(w_o[h_t, x_t] + b_t) \quad (15)$$

Updated Hidden State Equation

$$h_t = o_t \odot \tanh(C_t) \quad (16)$$

In this way, LSTM networks are capable of modeling long-range dependencies in sequential data, overcoming the limitations of traditional feedforward and basic RNN architectures. They are widely used for time series forecasting and sequence modeling with high efficiency and precision [28].

II.4 VAR-CHOLESKY METHOD

The Vector Autoregressive (VAR) method was introduced by Christopher A. Sims in 1980 through the publication Macroeconomics and Reality. It evolved from the autoregressive (AR) model and allows for the simultaneous modeling of lagged interdependencies among multiple time series. In this framework, all variables are treated as interdependent, eliminating the need to distinguish between dependent and independent variables [29]. However, the method presents some limitations, such as sensitivity to the number of lags chosen, which can lead to overparameterization or under parameterization.

Another limitation arises from the potential high dimensionality when the number of endogenous variables and lags is large, requiring a substantial amount of data [30]. Additionally, The VAR method assumes that the time series is stationary, meaning its statistical properties—such as mean, variance, and covariance—must remain constant over time [31]. In this study, STL decomposition is proposed to separate the trend and seasonality from the time series, with the expectation that the resulting residuals will be stationary.

The mathematical foundation of the VAR method is based on vectors and matrices. Vectors represent the values of the variables over time, while matrices contain the coefficients that describe variance and covariance among these variables across different time lags. This interaction is modeled through a linear equation, as presented in Equation 17 which captures the mutual influence among variables over time [31].

VAR Equation

$$Y_t = C + \sum_{i=1}^{p} \Phi_i \, Y_{t-1} + \epsilon_t \quad (17)$$

Where:
Y_t: vector of endogenous variables;
Φ_i: coefficient matrices;
C: constant vector;
ϵ_t: vector of error terms;
p: model order (number of lags).

Expanding this equation for all time periods with T observations, one can stack the equations corresponding to periods $t = p + 1$ to T into a matrix form, as shown in Equation 18. This reformulation allows all observations to be treated simultaneously, enabling a direct solution using the Ordinary Least Squares (OLS) method [32], [33].

Reduced VAR

$$Y = Z\Theta + E \quad (18)$$

Where:

Matrix of Dependent Variables (Y): Composed of transposed vectors of endogenous variables $Y_{p+1}^T, Y_{p+2}^T, \ldots, Y_T^T$, with dimensions $(T - p) \times N$;

Matrix of Constants and Lagged Variables (Z): Concatenates a vector of constants (C) and lagged endogenous variables, with dimensions $(T - p) \times (N \cdot p + 1)$;

Matrix of Coefficients (Θ): Composed of the transposed constant vector (C^T) and the coefficient matrices Φ_1 to Φ_p, with dimensions $(N \cdot p + 1) \times N$;

Matrix of Residuals (E): Organizes the transposed error terms ϵ^T from period $p + 1$ to T, with dimensions $(T - p) \times N$.

Equation 19 is derived by isolating the error matrix E from Equation 18 and substituting it into the minimization of the sum of squared residuals $S(\Theta) = E^T E$, according to the OLS method. Thus, $\widehat{\Theta}$ represents the theoretical coefficients that minimize $S(\Theta)$, corresponding to the values that minimize the squared error between observed and predicted values [32].

Least Squares VAR Equation

$$\widehat{\Theta} = (Z^T Z)^{-1} Z^T Y \tag{19}$$

By substituting $\widehat{\Theta}$ into Equation 18, one obtains the estimated residual matrix $\hat{E}$, which contains the differences between observed values and model-adjusted values for each of the $T - p$ periods. Then, Equation 20 can be applied to calculate the sample covariance matrix of the residuals, describing the variability and dependency structure among the residuals of the VAR model's endogenous variables [33].

Sample Covariance Matrix

$$\sum\nolimits_{\epsilon} = \frac{\hat{E}^T \hat{E}}{T - p} \tag{20}$$

Where:
$\widehat{\Sigma_\epsilon}$: estimated covariance matrix of the residuals;
T: total number of time periods;
$\widehat{E^T}$: transposed matrix of residuals.

This process captures the correlation, magnitude, and direction of the model residuals, where each element $\hat{\Sigma}_\epsilon^{ij}$ represents the covariance between residuals i and j. In this context, both the residual matrix and the residual covariance matrix provide a deep understanding of the unexplained component of the model. To incorporate this unexplained behavior into simulations, the Cholesky decomposition is applied to the covariance matrix of the residuals, as shown in Equation 21. This factorizes a symmetric positive definite matrix into the product of a lower triangular matrix and its transpose [34].

Cholesky Equation

$$\Sigma_\epsilon = LL^t \tag{21}$$

II.5 FINANCIAL MATHEMATICAL MODELING

The most fundamental concept for developing a financial mathematical model lies in understanding the concepts of revenue, fixed costs, variable costs, investment expenses, debt payments, and dividend distributions. These can be detailed as follows:

Cash Inflows [35]:

- Sales Revenue: Refers to income generated from product sales, with the amount received varying directly with the quantity of goods and services sold;
- Financial Revenues: Arise from financial activities, such as interest from investments, dividends on equity, foreign exchange gains, among others;
- Other Operating Revenues: These are part of the company's cash flow but are not related to its core business activities. Examples include rental income, proceeds from by-products, compensation received, etc.

Cash Outflows [36]:

- Fixed Costs: Recurring expenses necessary for maintaining the company’s operations that do not vary with production volume. Examples include rent, insurance, and salaries;
- Variable Costs: Costs directly related to the production volume, such as raw materials, supply expenses, and sales commissions;
- Investment Expenses: Expenditures on tangible or intangible assets aimed at generating future financial returns, such as spending on new projects, equipment, or capacity expansion;
- Financial Expenses: Costs related to debt service, such as loan repayments and interest payments.

These concepts are structured in various ways to report business performance. However, the cash flow statement and the balance sheet are the most basic tools for financial evaluation. The following sections briefly explain these tools, highlighting their main characteristics, advantages, and limitations. The cash flow (CF) statement is a financial tool that records all of the company’s cash inflows and outflows. It is divided into three categories: operating cash flow (OCF), investing cash flow (ICF), and financing cash flow (FCF), as expressed in Equation 22 [37].

Cash Flow Equation

$$\mathrm{CF}_t = \mathrm{OCF}_t + \mathrm{ICF}_t + \mathrm{FCF}_t \tag{22}$$

The OCF includes all financial movements related to the company’s core activities. It consists of both operating revenues and expenses. Revenues mainly stem from product and service sales, including by-product sales, freight charges, and additional services. Expenses include payments to suppliers, wages and payroll charges, infrastructure costs, taxes on sales, and commercial expenses [37]. This is modeled by Equation 23. If this indicator remains negative for extended periods, it threatens the company’s viability.

Operating Cash Flow Equation

$$\text{OCF}_t = \text{Operating Cash Inflows}_t - \text{Operating Cash Outflows}_t \quad (23)$$

The ICF accounts for financial movements involving the acquisition or disposal of long-term assets, including financial investments. Inflows originate from asset sales, proceeds from financial applications, or divestments. Outflows cover the purchase of machinery, buildings, participation in other businesses, and infrastructure investments [37]. According to Equation 24, a positive ICF indicates disinvestment, while a negative value suggests active long-term investment.

Investing Cash Flow Equation

$$\text{ICF}_t = \text{Investment Inflows}_t - \text{Investment Outflows}_t \quad (24)$$

The FCF relates to the company's financing activities and capital structure. Inflows include borrowed capital, equity issuance, or capital contributions from shareholders. Outflows include debt repayments, interest payments, dividend distributions, and share buybacks [37].

Financing Cash Flow Equation

$$\text{FCF}_t = \text{Financing Inflows}_t - \text{Financing Outflows}_t \quad (25)$$

While OCF and ICF are directly interpretable, FCF requires more nuanced analysis. A positive FCF indicates the company is taking on debt, which may be strategic if occasional (e.g., leveraged investment). However, recurring positive FCF values may indicate over-reliance on debt to sustain operations. A negative FCF typically reflects debt repayment and shareholder returns, often interpreted as a positive indicator.

II.6 FINANCIAL ANALYSIS TOOLS

Cash flow and the balance sheet form the basis for various financial analyses. Below are tools used to assess investment risks and project viability.

II.6.1 Net Present Value (NPV)

NPV calculates the difference between the present value of expected cash flows and the initial investment, as defined in Equation 26 [35].

Net Present Value Equation

$$\text{NPV} = \sum_{t=0}^{n} \frac{\text{CF}_t}{(1+i)^t} - I_0 \quad (26)$$

Where:
t: Time period;
CF_t: Cash flow in period t;
i: Discount rate or minimum acceptable rate of return;
I_0: Initial investment.

NPV yields three main interpretations for investment decisions: a positive NPV indicates financial viability, where the project's net income exceeds its cost; a negative NPV implies economic inviability; and an NPV close to zero suggests the investment merely breaks even [38]. When applied in Monte Carlo simulations, NPV is calculated for each generated scenario, allowing for statistical analysis across scenarios (mean, standard deviation, quartiles) [39].

II.6.2 Probability of Positive Return (PPR)

PPR is a probabilistic economic viability metric that evaluates the likelihood of a project yielding positive returns over a specified time horizon. Using stochastically generated scenarios, each case is evaluated for profitability (e.g., whether NPV > 0). The proportion of positive-return scenarios among all simulations is calculated, as shown in Equation 27 [40].

Probability of Positive Return Equation

$$\text{PPR} = \frac{\text{Number of Scenarios with Positive Return}}{\text{Total Number of Simulated Scenarios}} \quad (27)$$

II.6.3 Discounted Payback Period

The Discounted Payback Period estimates the time required to recover an investment, accounting for a discount rate. It is computed by identifying the minimum T where the cumulative present value of cash flows exceeds the initial investment, as shown in Equation 28 [41].

Discounted Payback Equation

$$\text{Discounted Payback} = \min\left\{T: \sum_{t=1}^{T} \frac{\text{CF}_t}{(1+i)^t} \geq I_0\right\} \quad (28)$$

In Monte Carlo simulations, this metric is applied to each individual scenario. Results are then statistically analyzed to derive metrics such as average payback time, standard deviation, and quartiles [40].

III. MATERIALS AND METHODS

The proposed conceptual model, as illustrated in Figure 1, is structured into three stages, classified according to the nature of their activities.

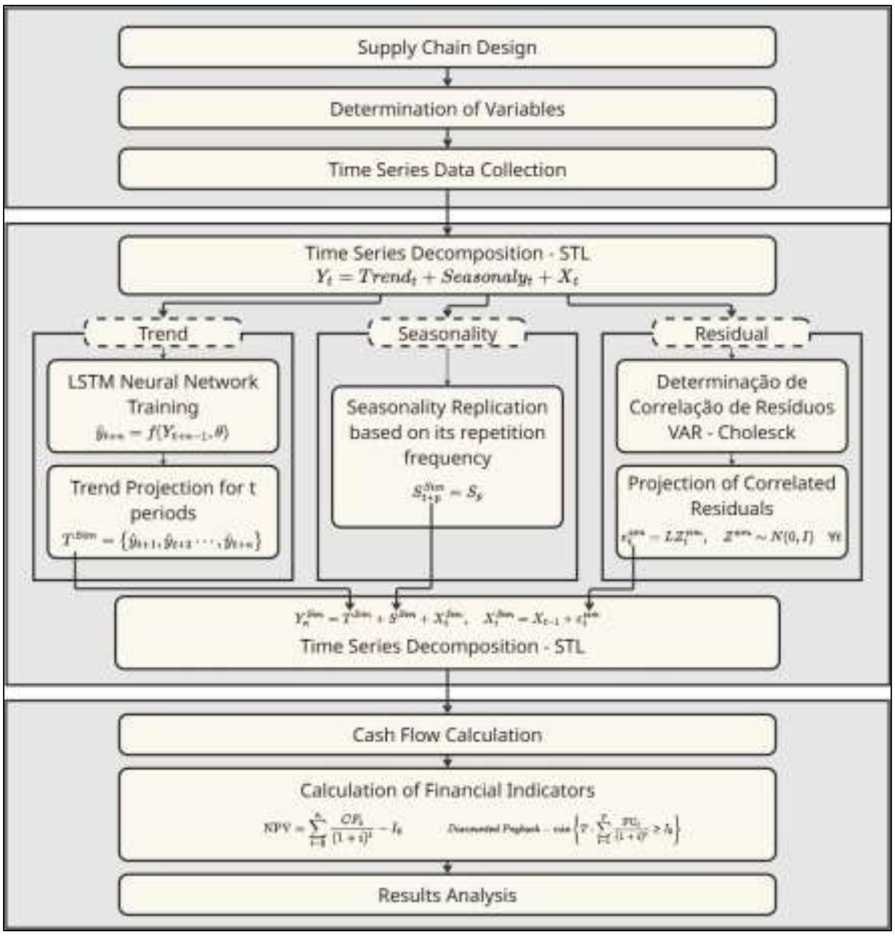

Figure 1: Conceptual Model.
Source: Authors, (2025).

III.1 PRODUCTION CHAIN

The first stage involves the design of the production chain to be analyzed. Although this work does not delve deeply into the theoretical basis of this step, a general overview is provided based on the evidence discussed in [6]. At least three different approaches can be used to structure this production chain:

III.1.1 Based on an existing supply chain

Analyzing existing supply chains is useful for business planning, as it enables incorporating validated strategies and empirical knowledge - a process commonly referred to as benchmarking. This approach is not limited to companies within the same industry as the target project but can also draw from firms in different sectors within the same region.

III.1.2 Based on expert opinion

Expertise should not be overlooked. Even with rigorous studies and sound project management methods, subtle nuances may be missed. Expert reviews help identify waste, challenges, design flaws, and other risks. Specialist consultation is also essential in adjacent areas, such as taxation, environmental regulations, and legal compliance.

III.1.3 Based on academic studies

Research-based development enables innovation in investment projects, whether related to product design or process improvement. Academic literature reviews and the synthesis of scholarly knowledge provide an innovative foundation that may help establish a competitive edge. Innovation is crucial for the success of new ventures that lack economies of scale or an established market. Without some form of product or process innovation, new companies often face severe market entry difficulties.

From this production chain layout, it is possible to identify the key project variables, including fixed costs, variable costs, revenues, and investments. Additional data may also be needed, such as historical inflation rates, currency exchange rates (e.g., USD), among others. Collecting these time series can be challenging and may require collaboration with companies or institutions, as access to such data is often restricted.

III.2 TIME SERIES FORECASTING

Once the production chain is defined and data collected, the model proceeds with the decomposition of time series using the STL method. As described for Reference 19 , STL decomposes each time series into trend, seasonal, and residual components in a unified manner. This joint decomposition is highly desirable. Applying different methods to extract each component separately introduces different parameters and biases, potentially resulting in overlap between trend and residual components. STL's unified decomposition improves model stability by avoiding such issues. Another advantage of STL is its ability to produce stationary residuals, which is crucial for analyzing residual correlation. Verifying stationarity is essential and should be done using tests such as the Dickey-Fuller Test, KPSS Test, and Phillips-Perron Test. If residuals are found to be non-stationary, STL parameters can be adjusted and reapplied, avoiding the need for additional transformations such as differencing, log transformations, or the Box-Cox transformation - which may be methodologically costly and risk information loss, ultimately reducing model robustness. After decomposition, the model separately forecasts each of the three components.

Trend forecasting is performed using Long Short-Term Memory (LSTM) neural networks, chosen for their capacity to capture both long- and short-term dependencies in financial time series [42]. Prior to training, the time series data undergoes preprocessing. A common step is normalization, which scales values to a 0–1 range, preventing large-scale numbers from disproportionately influencing training [43]. Another preprocessing step involves converting dates into sequential integers. For example, neural networks may struggle to interpret the transition from month 12 (December 2024) to month 01 (January 2025). Using sequential numeric encoding and reverting it during postprocessing improves interpretability. Additionally, a cyclical temporal component, such as a sine or cosine function, can be included to help the network detect seasonal patterns not fully captured by STL [44], [45].

During network configuration, key parameters must be defined:

- Batch size: number of samples processed simultaneously.
- Timesteps: length of time intervals processed as a unit.
- Features: number of correlated variables used as input.

LSTM architecture parameters include:

- Number of units: neurons per layer;
- Activation functions: typically tanh and sigmoid;
- Number of layers;
- Dropout rate: to prevent overfitting by randomly disabling neurons during training.]

Training parameters (also known as learning parameters) include the definition of training, validation, and test sets, as well as:

- Loss function: measures the difference between predicted and actual values;
- Optimizer: updates weights and biases based on the loss.

Let T be a trend vector composed of x values over n time periods, as in Equation 29:

Trend Original Vector

$$T = \{x_{t-n}, x_{t-n+1}, \cdots, x_{t-1}, x_t\} \tag{29}$$

This vector T is input into an LSTM network, which forecasts the trend's future trajectory by iteratively adjusting weights and biases via the internal operations of the LSTM cell. These are represented by Equations 11, 12, 14, and 15, involving forget gate (f_t), input gate (i_t), output gate (o_t), and cell state update (C_y).

Two common issues may arise during training:

- Overfitting: the model memorizes patterns specific to the training data but fails to generalize;
- Underfitting: the model fails to capture meaningful patterns.
- These are mitigated by fine-tuning the above parameters \cite{li2024keeping}.

The forecast for the next time step is given by Equation 30:

LSTM Forecast Equation

$$\hat{y}t + n = f(Yt + n - 1, \theta) \tag{30}$$

Where:

- $\hat{y}t + n$: Forecasted value for period $t + n$;
- $Yt + n - 1$: Vector of previous values, including both actual and predicted data;
- f: Function learned by the LSTM network;
- θ: Parameters (weights and biases) of the trained model.

After training is complete, the model forecasts the full trend sequence over n periods, as shown in Equation 31:

Trend Projection Vector

$$\mathrm{T}^{Sim} = \{\hat{y}t + 1, \hat{y}t + 2 \cdots, \hat{y}t + n\} \tag{31}$$

III.3 SEASONALITY FORECASTING

As previously mentioned in Section II.2, the STL decomposition method produces a well-defined seasonality pattern, which facilitates the extrapolation of this periodic behavior into future cycles. Delving deeper into the seasonality projection methodology, after the time series is decomposed, each seasonal component S_t is associated with a corresponding time point t within the cycle. The cycle length P defines the number of seasonal values in a full cycle for monthly series with yearly seasonality. The seasonal pattern is represented by a sequence of P values, $S = \{S_1, S_2, \dots, S_P\}$, where each value corresponds to a specific position within the cycle. For future time points $t > T$, where T is the last observed value of the series, seasonality is projected using Equation 32 [21].

Forecasted Seasonal Value Equation

$$S_{t+p} = S_p \tag{32}$$

Where:

S_{t+p}: forecasted seasonal value;
S_p: value from the seasonal cycle, with p ranging from 1 to P.

In cases where seasonality exhibits non-stationary behavior, regression-based models may be applied to dynamically adjust the amplitude of seasonal components over time [46].

III.4 RESIDUAL FORECASTING

The VAR-Cholesky method was selected for modeling the correlation between residuals due to its ability to capture interdependencies among multiple time series, including time lags [47]. This characteristic is essential for generating robust feasibility forecasts. To illustrate the importance of properly identifying correlation among series, consider a yogurt manufacturing plant. One can reasonably expect a correlation between the price of raw milk (a commodity) and the final price of yogurt. These prices may be influenced by external factors not fully captured in the model, the residuals. If residual correlations are ignored, the simulation may generate inconsistent results, where one variable fluctuates independently of the other, leading to unreliable viability projections.

Residual forecasting begins by applying the Monte Carlo method as described in Section II.4, resulting in the residual correlation matrix L. This matrix is multiplied by a standardized random variable vector (Z^{sim}), producing a simulated residual vector (ε_t^{sim}) for each period t. This process is repeated for T periods to cover the desired simulation horizon. The results for all simulations can be stored in a residual simulation matrix E^{sim} with dimensions $N \times T$ [48].

Residual Forecasting Equation

$$\varepsilon_t^{sim} = L Z_t^{sim}, \quad Z^{sim} \sim N(0, I) \quad \forall t \tag{33}$$

These results are equivalent to white noise (as in Equation 1) but now incorporating the correlation among time series residuals. By applying Equation 33 to the Brownian noise formulation in Equation 2, the behavior of the residual component in the simulations is fully defined. This process is repeated N times to generate the desired number of Monte Carlo scenarios [18], [49].

III.5 RECONSTRUCTION OF FORECASTED TIME SERIES

After decomposition using the STL method, reconstruction of the forecasted time series is a simple process involving the sum of the trend, seasonal, and residual components. This is represented by Equation 34, where n denotes the simulation index [19].

Forecasted Time Series Equation

$$Y^{Sim} = T^{Sim} + S^{Sim} + Xn^{Sim} \tag{34}$$

It is important to note that the trend and seasonal components can be treated as constant across all simulations. In other words, their values remain fixed, while the residuals are resampled for each simulation scenario. This separation is computationally efficient: although training the LSTM network and computing autoregressive vectors is resource-intensive, the subsequent steps involve only first-order arithmetic operations.

IV. RESULTS AND DISCUSSIONS

The evaluation of investment risk begins with the mathematical modeling of cash flow, as represented by the simplified Equation 35.

Cash Flow Equation

$$\text{FC}_t = \text{Revenues}_t - \text{Fixed Costs}_t - \text{Variable Costs}_t \tag{35}$$

By applying the forecasted time series to this cash flow equation, we obtain a cash flow projection for each period t and each of the n simulated scenarios. These projected cash flows are then analyzed using investment evaluation tools such as Net Present Value (NPV) and Discounted Payback Period [38], [41]. Since the results are based on a set of simulated scenarios, they can be subjected to statistical analysis.

For example, calculating the lower quartile of NPV yields the Value at Risk (VaR), representing the greatest expected loss at a given confidence level (typically 5% or 1%). Additionally, by counting the number of scenarios in which the NPV is greater than zero, one obtains the probability of positive returns. From the Discounted Payback results, it is possible to estimate the average time to investment recovery, as well as determine the expected return periods in worst-case scenarios [40].

V. CONCLUSIONS

This study introduced a conceptual method for risk assessment in manufacturing investments, contributing with a novel approach that integrates STL, LSTM, and VAR-Cholesky methods to forecast correlated time series of costs and revenues. The model advances investment analysis techniques from both an economic science and a production engineering perspective. While theoretically robust, the model's practical utility must be confirmed through empirical validation in real-world case studies. The primary limitations of the current framework are the unstructured nature of the production chain modeling and the absence of an optimization module. Future work should therefore focus on two key areas: first, developing a more rigorous and detailed modeling process for a generic production chain; and second, incorporating an optimization layer to identify ideal investment strategies. Successfully addressing these points will enhance the model's applicability, potentially establishing it as a valuable tool for feasibility analysis and risk forecasting in the manufacturing sector.

VI. AUTHOR'S CONTRIBUTION

Conceptualization: Rafael Vieira da Silva, Enzo Morosini Frazzon.
Methodology: Rafael Vieira da Silva, Enzo Morosini Frazzon.
Investigation: Rafael Vieira da Silva, Enzo Morosini Frazzon.
Discussion of results: Rafael Vieira da Silva, Enzo Morosini Frazzon
Writing – Original Draft: Rafael Vieira da Silva, Enzo Morosini Frazzon
Writing – Review and Editing: Rafael Vieira da Silva, Enzo Morosini Frazzon
Resources: Rafael Vieira da Silva, Enzo Morosini Frazzon
Supervision: Rafael Vieira da Silva, Enzo Morosini Frazzon
Approval of the final text: Rafael Vieira da Silva, Enzo Morosini Frazzon

VII. ACKNOWLEDGMENTS

This work was carried out with the support of the Coordination for the Improvement of Higher Education Personnel – Brazil (CAPES) – Financing Code 88887.877819/2023-00

VIII. REFERENCES

[1] H. Wang and Z. Zhou, "Identification of key risk nodes and invulnerability analysis of construction supply chain networks," Buildings, vol. 14, no. 7, p. 1997, 2024.

[2] S. DuHadway, S. Carnovale, and B. Hazen, "Understanding risk management for intentional supply chain disruptions: Risk detection, risk mitigation, and risk recovery," Annals of Operations Research, vol. 283, pp. 179–198, 2019.

[3] T. S. Oliveira, C. V. B. Júnior, and M. Caetano, "Return on investing in innovative activities: the brazilian manufacturing industry," International Journal of Innovation, vol. 11, no. 1, pp. e22797–e22797, 2023.

[4] I. Zykiene, A. Leskauskien, I. Miciulien, and R. Dauglien, "Driving Growth and Innovation: Exploring Foreign Direct Investment in the Manufacturing Sector (The Case of Lithuania)," European Integration Studies, no. 17, pp. 124–140, 2023.

[5] N. F. Silva, M. dos Santos, C. F. S. Gomes, and L. P. de Andrade, "An integrated CRITIC and Grey Relational Analysis approach for investment portfolio selection," Decision Analytics Journal, p. 100285, 2023.

[6] R. V. ạ Silva and E. M. Frazzon, "ESTADO DA ARTE DOS MÉTODOS PARA ANÁLISE DE VIABILIDADE ECONÔMICA NA INDÚSTRIA DE TRANSFORMAÇÃO," Gestão Da Produção, Operações E Sistemas, 2025.

[7] J. Zhang, "Modern Monte Carlo methods for efficient uncertainty quantification and propagation: A survey," Wiley Interdisciplinary Reviews: Computational Statistics, vol. 13, no. 5, p. e1539, 2021.

[8] B. H. Gebreslassie, Y. Yao, and F. You, "Design under uncertainty of hydrocarbon biorefinery supply chains: multiobjective stochastic programming models, decomposition algorithm, and a comparison between CVaR and downside risk," AIChE Journal, vol. 58, no. 7, pp. 2155–2179, 2012.

[9] S. L. Ngan, B. S. How, S. Y. Teng, W. D. Leong, A. C. M. Loy, P. Yatim, M. A. B. Promentilla, and H. L. Lam, "A hybrid approach to prioritize risk mitigation strategies for biomass polygeneration systems," Renewable and Sustainable Energy Reviews, vol. 121, p. 109679, 2020.

[10] T. Ingelaere, V. Maes, and G. Samaey, "Cell Escape Probabilities for Markov Processes on a Grid," arXiv preprint arXiv:2404.00314, 2024.

[11] W. Li, M. Lu, and P. Ye, "Optimal restricted Monte Carlo integration on generalized Hölder classes," Journal of Applied Mathematics and Computing, pp. 1–26, 2025.

[12] J. Yoder, C. Alexander, R. Ivanic, S. Rosch, W. Tyner, and S. Wu, "Risk Versus Reward, a Financial Analysis of Alternative Contract Specifications for the Miscanthus Lignocellulosic Supply Chain," BioEnergy Research, vol. 8, 2015.

[13] I.-W. G. Kwon and T. Suh, "Trust, commitment and relationships in supply chain management: a path analysis," Supply chain management: an international journal, vol. 10, no. 1, pp. 26–33, 2005.

[14] W. Tian, Y. Heo, P. de Wilde, Z. Li, D. Yan, C. S. Park, X. Feng, and G. Augenbroe, "A review of uncertainty analysis in building energy assessment," Renewable and Sustainable Energy Reviews, vol. 93, pp. 285–301, 2018.

[15] V. Platon and A. Constantinescu, "Monte Carlo Method in Risk Analysis for Investment Projects," Procedia Economics and Finance, vol. 15, pp. 393–400, 2014.

[16] P. Capuozzo, E. Panella, T. S. Gherardini, and D. D. Vvedensky, "Path integral Monte Carlo method for option pricing," Physica A: Statistical Mechanics and its Applications, vol. 581, p. 126231, 2021.

[17] M. West, “Time series decomposition,” Biometrika, vol. 84, no. 2, pp. 489–494, 1997.

[18] L. Heinäkoski, “Limitations of normal distribution in economic risk analysis,” L. Heinäkoski, 2018.

[19] T. Krake, D. Klötzl, D. Hägele, and D. Weiskopf, “Uncertainty-Aware Seasonal-Trend Decomposition Based on Loess,” IEEE Transactions on Visualization and Computer Graphics, 2024.

[20] F. Leite Coelho da Silva, J. da Silva Cordeiro, K. da Costa, N. Saboya, P. Canas Rodrigues, and J. L. López-Gonzales, “Time series forecasting via integrating a filtering method: an application to electricity consumption,” Computational Statistics, pp. 1–20, 2025.

[21] T. Phungtua-eng and Y. Yamamoto, “Adaptive Seasonal-Trend Decomposition for Streaming Time Series Data with Transitions and Fluctuations in Seasonality,” in Joint European Conference on Machine Learning and Knowledge Discovery in Databases, 2024, pp. 426–443.

[22] K. Zhang, X. Huo, and K. Shao, “Temperature Time Series Prediction Model Based on Time Series Decomposition and Bi-LSTM Network,” Mathematics, vol. 11, no. 9, 2023.

[23] E. S. Gardner Jr and E. McKenzie, “Forecasting trends in time series,” Management science, vol. 31, no. 10, pp. 1237–1246, 1985.

[24] D. E. Rumelhart, G. E. Hinton, and R. J. Williams, “Learning representations by back-propagating errors,” nature, vol. 323, no. 6088, pp. 533–536, 1986.

[25] C. L. Giles, D. Chen, G.-Z. Sun, H.-H. Chen, Y.-C. Lee, and M. W. Goudreau, “Constructive learning of recurrent neural networks: limitations of recurrent cascade correlation and a simple solution,” IEEE Transactions on Neural Networks, vol. 6, no. 4, pp. 829–836, 1995.

[26] S. Hochreiter and J. Schmidhuber, “LSTM can solve hard long time lag problems,” Advances in neural information processing systems, vol. 9, 1996.

[27] J. Schmidhuber, S. Hochreiter, and others, “Long short-term memory,” Neural Comput, vol. 9, no. 8, pp. 1735–1780, 1997.

[28] Y. Yu, X. Si, C. Hu, and J. Zhang, “A review of recurrent neural networks: LSTM cells and network architectures,” Neural computation, vol. 31, no. 7, pp. 1235–1270, 2019.

[29] C. A. Sims, “Macroeconomics and reality,” Econometrica: journal of the Econometric Society, pp. 1–48, 1980.

[30] J. H. Stock and M. W. Watson, “Vector autoregressions,” Journal of Economic perspectives, vol. 15, no. 4, pp. 101–115, 2001.

[31] F. Canova, “Vector autoregressive models: specification, estimation, inference, and forecasting,” Handbook of applied econometrics volume 1: Macroeconomics, pp. 53–110, 1999.

[32] K. Kavaklioglu, “Principal components based robust vector autoregression prediction of Turkey’s electricity consumption,” Energy Systems, vol. 10, no. 4, pp. 889–910, 2019.

[33] P. Kohli, T. P. Garcia, and M. Pourahmadi, “Modeling the Cholesky factors of covariance matrices of multivariate longitudinal data,” Journal of Multivariate Analysis, vol. 145, pp. 87–100, 2016.

[34] H. Lütkepohl, “Vector autoregressions,” Companion to Theoretical Econometrics, Blackwell, Oxford, pp. 678–699, 2001.

[35] G. Lucko, “Supporting financial decision-making based on time value of money with singularity functions in cash flow models,” Construction Management and Economics, vol. 31, no. 3, pp. 238–253, 2013.

[36] S. Briciu, “Variable and fixed costs in company management,” Annales Universitatis Apulensis Series Oeconomica, vol. 1, no. 10, pp. 1–14, 2008.

[37] K. Simons, “The relationship between dividend changes and cash flow: An empirical analysis,” Journal of Business Finance & Accounting, vol. 21, no. 4, pp. 577–587, 1994.

[38] T. Shou, “A literature review on the net present value (NPV) valuation method,” in 2022 2nd International Conference on Enterprise Management and Economic Development (ICEMED 2022), 2022, pp. 826–830.

[39] S. S. Shaffie and S. H. Jaaman, “Monte Carlo on net present value for capital investment in Malaysia,” Procedia-Social and Behavioral Sciences, vol. 219, pp. 688–693, 2016.

[40] I. M. Ronyastra, L. H. Saw, and F. S. Low, “Monte Carlo simulation-based financial risk identification for industrial estate as post-mining land usage in Indonesia,” Resources Policy, vol. 89, p. 104639, 2024.

[41] A. Kijo-Kleczkowska, P. Brus, and G. Wikeciorkowski, “Profitability analysis of a photovoltaic installation - A case study,” Energy, vol. 261, p. 125310, 2022.

[42] A. Sunki, C. SatyaKumar, G. S. Narayana, V. Koppera, and M. Hakeem, “Time series forecasting of stock market using ARIMA, LSTM and FB prophet,” in MATEC Web of Conferences, 2024, vol. 392, p. 01163.

[43] H. Agarwal, G. Mahajan, A. Shrotriya, and D. Shekhawat, “Predictive Data Analysis: Leveraging RNN and LSTM Techniques for Time Series Dataset,” Procedia Computer Science, vol. 235, pp. 979–989, 2024.

[44] C. Arthur, N. Yudistira, and C. Dewi, “AutoCyclic: Deep Learning Optimizer for Time Series Data Prediction,” IEEE Access, 2024.

[45] F. Zhang, M. Wang, W. Zhang, and H. Wang, “THATSN: Temporal hierarchical aggregation tree structure network for long-term time-series forecasting,” Information Sciences, vol. 692, p. 121659, 2025.

[46] M. K. P. So and R. S. W. Chung, “Dynamic seasonality in time series,” Computational Statistics & Data Analysis, vol. 70, pp. 212–226, 2014.

[47] M. Demetrescu and N. Salish, “(Structural) VAR models with ignored changes in mean and volatility,” International Journal of Forecasting, vol. 40, no. 2, pp. 840–854, 2024.

[48] J.-S. Chou, “Cost simulation in an item-based project involving construction engineering and management,” International Journal of Project Management, vol. 29, no. 6, pp. 706–717, 2011.

[49] D. J. Higham and M. Roj, “Computing mean first exit times for stochastic processes using multi-level Monte Carlo,” in Proceedings of the 2012 Winter Simulation Conference (WSC), 2012, pp. 1–10.